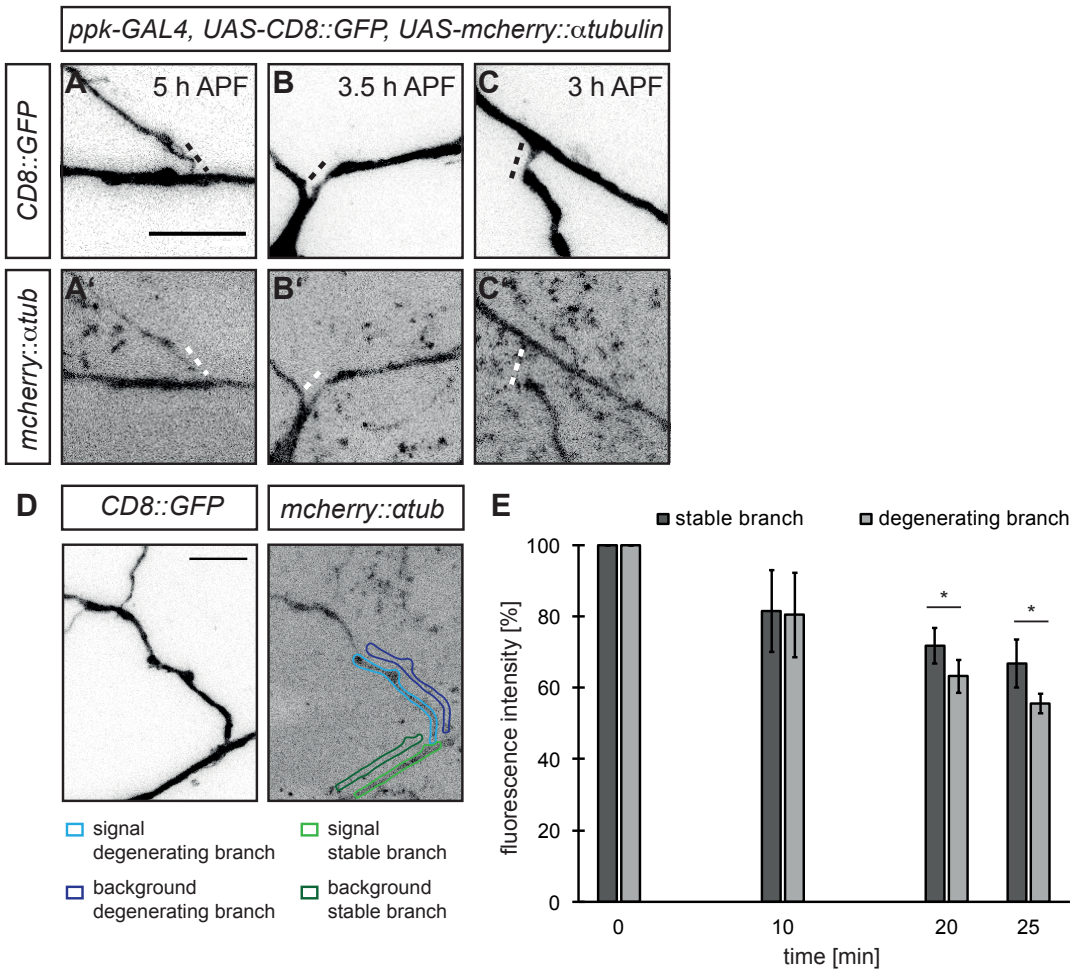

Fig. S1 related to Fig. 1. Microtubule loss at dendritic branch points.

A - C' Representative example images of CD8::GFP (A-C) and mcherry::αtubulin (A'-C') showing thinning of dendritic membranes and microtubule loss starting at branch points at the indicated time points after puparium formation (APF). Dashed lines indicate thinned regions with microtubule loss. **D, E** Quantification of microtubule loss at branch points. Relative mcherry::αtubulin fluorescence intensity was measured in degenerating as well as adjacent stable branches for control. **D** Schematic showing example areas for measurements of signal versus background. The mean intensities were measured in areas within the stable (light green) as well as the degenerating branch (light blue) and the background intensities of flanking regions (dark green and dark blue) were subtracted. The start values were set to 100 %. **E** Graph showing fluorescence loss of mcherry::αtubulin in stable and degenerating branches over a 25 minute time period starting at times when mcherry::αtubulin signal in degenerating branches was still continuous (N = 13 for each time point). * $P<0.05$ (using Wilcoxon's test). Data are means ± SD. The scale bars are 10 μm.

Development • Supplementary information

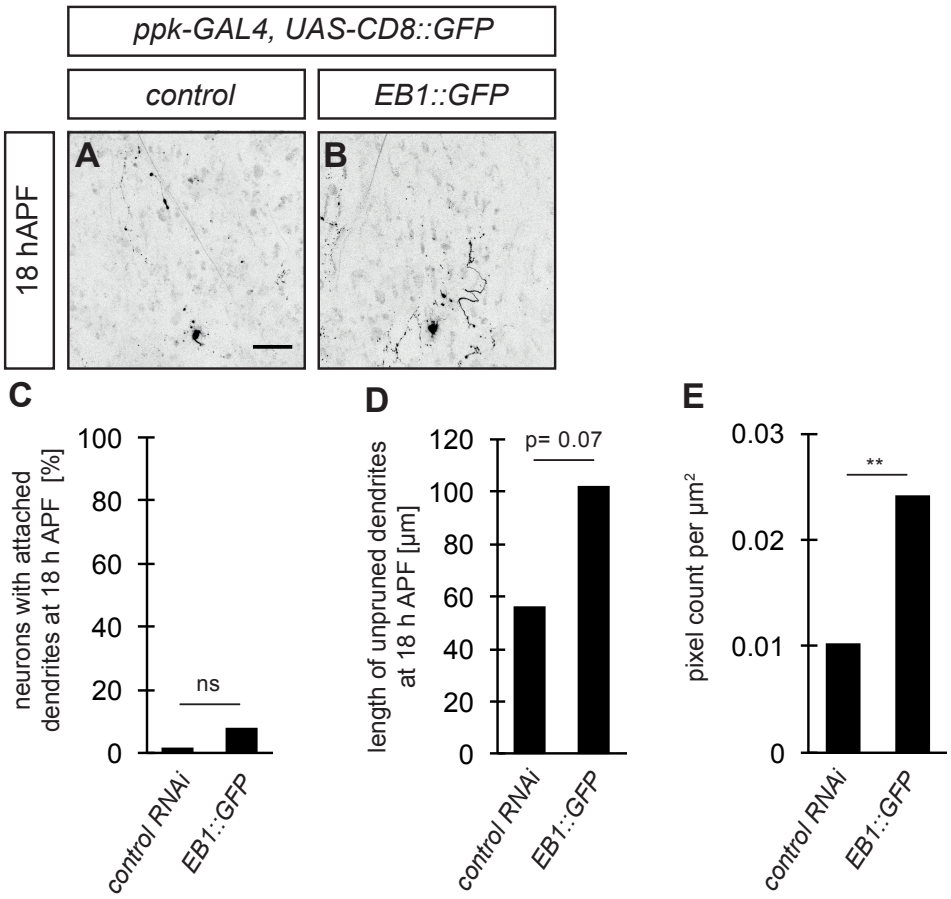

Fig. S2 related to Fig. 3. Mild pruning defects caused by overexpression of EB1::GFP.

A, B Overexpression of EB1:GFP leads to mild pruning defects at 18 h APF. **C - E** Quantification of pruning defect. **C** Percentage of neurons with attached dendrites to the soma at 18 h APF. **D** Length of unpruned dendrites at 18 h APF. **E** Remaining dendritic signal shown as pixel count per area. Z-axis maximum projections of confocal stacks were converted to binary images using the thresholding with MaxEntropy method in Fiji. Rectangular regions of interest were drawn within the dendrite area and the number of pixels within this area was measured (E). (N= 55 and 64 respectively)

** P<0.005 (using Wilcoxon's test). The scale bar is 50 μm.

Development • Supplementary information

A

	retrograde	anterograde	N	P
control	96 %	4 %	53	
khc^{mutA}	90 %	10 %	39	ns

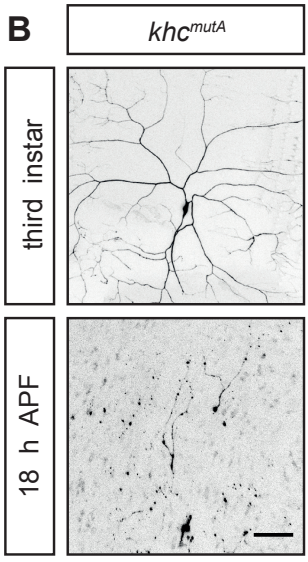

Fig. S3 related to Fig. 5. Effect of *khc^{mutA}* on dendritic microtubule orientation and dendrite pruning.

A EB1::GFP was expressed in *khc^{mutA}* mutants under the control of ppk-GAL4. Microtubule orientation in c4da neurons was followed by tracking of comets in third instar proximal dendrites. The table summarizes the percentage of retrograde and anterograde comets. N is the number of comets analyzed (The control is the same as in main Figure 2). Significance was assessed using Fisher's exact test. **B** *khc^{mutA}* mutants only show a mild pruning defect (14 % with dendrites attached to the cell body at 18 h APF). Scale bar is 50 µm.

Development • Supplementary information

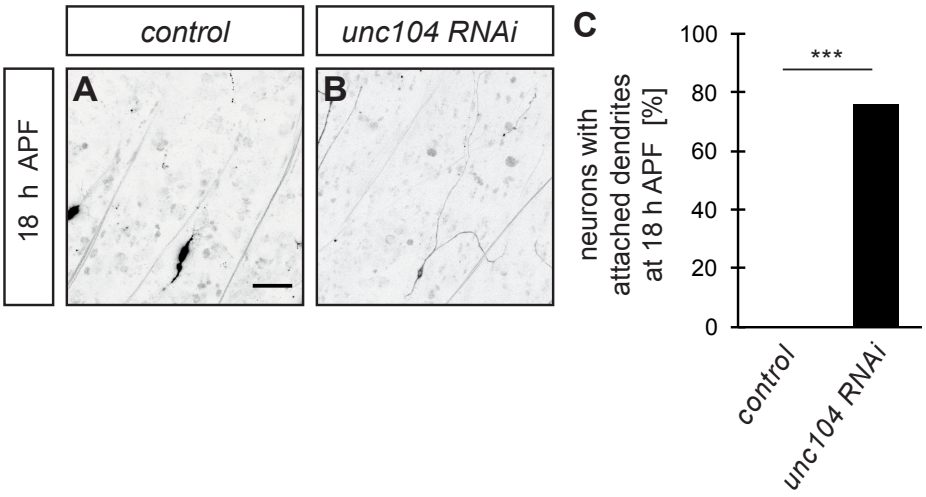

Fig. S4 related to Fig. 5. Pruning defects caused by unc104 knockdown.

A, B control c4da neurons (A) or c4da neurons expressing unc104 RNAi (B) under control of ppk-GAL4 were imaged at 18 h APF. **C** Quantification of pruning defects in A and B. *** $p<0.0005$ Fisher's exact test, N=25 each

Development • Supplementary information

Table S1. List of experimental genotypes for all figures.

Figure	Panel	Genotype
1	A - I	*ppk-GAL4, UAS-CD8::GFP, UAS-mcherry::αtubulin*
2	A, B	*(1) GAL4$^{109(2)80}$, UAS-tdtomato; UAS-EB1-GFP, UAS-dcr2* *(2) GAL4$^{109(2)80}$, UAS-tdtomato; UAS-EB1-GFP, UAS-dcr2, UAS-kap3 RNAi (VDRC3260)* *(3) GAL4$^{109(2)80}$, UAS-tdtomato; UAS-EB1-GFP, UAS-dcr2, UAS-par-1 RNAi (BL32410)*
2	C	*(1) ppk-GAL4, UAS-CD8::GFP, UAS-kinlacZ* *(2) ppk-GAL4, UAS-CD8::GFP, UAS-kinlacZ, UAS-kap3 RNAi; UAS-dcr2* *(3) ppk-GAL4, UAS-CD8::GFP, UAS-kinlacZ, UAS-par-1 RNAi, UAS-dcr2*
3	A - C	*(1) ppk-GAL4, UAS-CD8::GFP (X, II), UAS-dcr2* *(2) ppk-GAL4, UAS-CD8::GFP (X, II), UAS-dcr2, UAS-kap3 RNAi* *(3) ppk-Gal4, UAS-CD8::GFP (II), klp64D^{n123}/klp64D^{k1}*
3	F - H	*(1) ppk-GAL4, UAS-CD8::GFP (X, II), UAS-dcr2, UAS-eb1 RNAi (VDRC 24451)* *(2) ppk-GAL4, UAS-CD8::GFP (X, II), UAS-dcr2, UAS-par-1 RNAi, UAS-orco RNAi* *(3) ppk-GAL4, UAS-CD8::GFP (X, II), UAS-dcr2, UAS-par-1 RNAi, UAS-eb1 RNAi*
4	A - D	*ppk-GAL4, UAS-CD8::GFP, UAS-mcherry::αtubulin, klp64D^{n123}/klp64D^{k1}*
4	E, F	*(1) ppk-GAL4, UAS-CD8::GFP (X, II), UAS-dcr2* *(2) ppk-GAL4, UAS-CD8::GFP (X, II), UAS-dcr2, UAS-kap3 RNAi*
5	A - C	*(1) SOP-FLP (X); FRTG13, tubGal80/FRTG13 khc^{27} ; R57C10-GAL4, UAS-tdtomato, ppk-eGFP (heterozygous non-MARCM clone as control, visualized by ppk-eGFP in the same animal)* *(2) SOP-FLP (X); FRTG13, khc^{27}; R57C10-GAL4, UAS-tdtomato, ppk-eGFP (homozygous MARCM clone, identified by tdtomato fluorescence)* *(3) SOP-FLP (X); FRTG13, khc^{27}; R57C10-GAL4, UAS-tdtomato, UAS-GFP::KHC (homozygous MARCM clone, GFP::KHC rescue)*
6	A, B	*(1) ppk-GAL4, UAS-CD8::GFP, UAS-kinlacZ* *(2) SOP-FLP (X); FRTG13, khc^{27}; R57C10-GAL4, UAS-tdtomato, UAS-kin::lacZ (homozygous MARCM clone expressing kinlacZ)*
6	C, D	*SOP-FLP (X); FRTG13, khc^{27}; R57C10-GAL4, UAS-tdtomato, UAS-EB1::GFP (homozygous MARCM clone expressing EB1::GFP)*
6	E, F	*(1) ppk-GAL4, UAS-tdtomato, UAS-GFP::αtubulin* *(2) SOP-FLP (X); FRTG13, khc^{27}; R57C10-GAL4, UAS-tdtomato, UAS-GFP::αtubulin (homozygous MARCM clone expressing GFP::αtubulin)*
6	G	*SOP-FLP (X); FRTG13, khc^{27}; R57C10-GAL4, UAS-tdtomato, ppk-eGFP (homozygous MARCM clone)*
6	H	*(1) ppk-GAL4, UAS-CD8::GFP, UAS-dcr2; UAS-par-1 RNAi* *(2) ppk-GAL4, UAS-CD8::GFP, UAS-dcr2; khc^{27}/+* *(3) ppk-GAL4, UAS-CD8::GFP, UAS-dcr2, UAS-par-1 RNAi, khc^{27}/+*